ISSN: 2538-2152; ECOPERSIA 2025;13(3): 287-303.

Tarbiat Modares University

Chaotic Analysis of Streamflow Dynamics through Dynamical Systems Theory: A Case Study of the Gilvan Sub-Watershed, Iran

ARTICLEINFO

Article Type
Original Research

Authors
Zahra Abdollahi, *Ph.D.*[1*]
Hassan Shadman, *Ph.D.*[2]
Rahim Kazemi, *Ph.D.*[3]
Ghobad Rostamizad, *Ph.D.*[1]

How to cite this article
Abdollahi Z., Shadman H., Kazemi R., Rostamizad Gh. Chaotic Analysis of Streamflow Dynamics through Dynamical Systems Theory: A Case Study of the Gilvan Sub-Watershed, Iran. ECOPERSIA 2025;13(3): 287-303.

DOI:
10.22034/ECOPERSIA.13.3.287

[1] Assistant Professor, Soil Conservation and Watershed Management Research Department, Zanjan Agricultural and Natural Resources Research and Education Center, AREEO, Zanjan, Iran.
[2] Ph.D., Soil Conservation and Watershed Management Research Department, Zanjan Agricultural and Natural Resources Research and Education Center, AREEO, Zanjan, Iran.
[3]Associate Professor, Soil Conservation and Watershed Management Research Institute, Agricultural Research, Education and Extension Organization (AREEO), Tehran, Iran.

*** Correspondence***
Address: 5th km, Airport Road, Zanjan, Iran
Tel: +989124420240
Email: z.abdollahi@areeo.ac.ir

Article History
Received: June 9, 2025
Accepted: August 10, 2025
Published: August 19, 2025

ABSTRACT

Aims: Understanding the dynamic nature of river discharge is essential for effective water management, particularly in regions subject to climatic and hydrological variability. This study applies chaos theory to detect nonlinear patterns in the monthly discharge of the Gilvan Sub-Watershed, a tributary of the Qezel Ozan River in northwestern Iran, integrating spectral noise diagnostics with implications for adaptive management.

Materials & Methods: Monthly discharge data (1963–2017) from the Gilvan hydrometric station were analyzed using phase space reconstruction. Optimal parameters—time delay of 2 months (Average Mutual Information) and embedding dimension of 6 (False Nearest Neighbors)—were applied. The correlation dimension was estimated using the Grassberger–Procaccia algorithm, and the largest Lyapunov exponent was computed to assess system sensitivity.

Findings: A significant decreasing trend in streamflow ($p < 0.001$) was detected, averaging 0.16 $m^3.s^{-1}month^{-1}$ over the study period. The correlation dimension (2.3) indicated a low-dimensional attractor, while the positive largest Lyapunov exponent (0.08) confirmed sensitivity to initial conditions, a hallmark of chaos. These results suggest that streamflow dynamics are shaped by variable precipitation, snowmelt, evaporation, and anthropogenic factors.

Conclusion: The presence of chaos implies fundamental limits to long-term predictability and supports the need for nonlinear modeling in water management. Recognizing such complexity is vital for sustainable resource planning under changing climatic conditions. However, this study did not explicitly assess the mechanical effects of dams or other hydraulic infrastructure, and its findings may be influenced by data quality and spatial coverage—issues that warrant further investigation.

Keywords: Chaos Theory; Lyapunov Exponent; Nonlinear Hydrology; River Discharge.

CITATION LINKS

[1] Albostan A., Önöz B. Implementation of c... [2] Mihailović D.T., Malinović-Milićević S.,... [3] Baggaley N.J., Langan S.J., Futter M.N.,... [4] Martínez J.H., Lehnertz K., Rubido N. In... [5] Zhao Y., Zhu T., Zhou Z., Cai H., Cao Z.... [6] Baker G.L., Gollub J.P. Chaotic dynamics... [7] Cunico I., Bertoldi W., Caponi F., Dijks... [8] Li T., Lan T., Zhang H., Sun J., Xu C.-Y... [9] Sivakumar B. Chaos theory in hydrology: ... [10] Ghorbani M.A., Kisi O., Aalinezhad M. A ... [11] Khatibi R., Sivakumar B., Ghorbani M.A.,... [12] Zounemat-Kermani M. Investigating chaos ... [13] Ogunjo S., Olusola A., Fuwape I., Durowo... [14] Rezaie H., Garebaghi P., Khani Temeliyeh... [15] Rolim L.Z.R., de Souza Filho F.A. Explor... [16] Kavian A., Dodangeh S., Abdollahi Z. Ann... [17] Avarand Y., Janatrostami S., Ashrafzadeh... [18] Najafi M.S., Alizadeh O. Climate zones i... [19] Zareian M.J., Seraj Ebrahimi R., Dehban ... [20] Ghorbani A., Moameri M., Dadjou F., Seye... [21] Benmebarek S., Chettih M. Chaotic analys... [22] Kostelich E.J., Schreiber T. Noise reduc... [23] Priestley M.B. The spectral analysis of ... [24] Brockwell P.J., Davis R.A. Introduction ... [25] Bloomfield, P. Fourier analysis of time ... [26] Asakereh H. Power spectrum analysis of t... [27] Cryer J.D. Chan K.S. Time series analysi... [28] Lin H. Nonlinear dynamic Process of fluv... [29] Takens F. Detecting strange attractors i... [30] Pari Zangeneh M., Ataei M., Moallem P. P... [31] Kennel M.B., Brown R., Abarbanel H.D.I. ... [32] Vallejo J.C., Sanjuan M.A.F. Predictabil... [33] Elshorbagy A., Simonovic S.P., Panu U.S.... [34] Kantz H., Schreiber T. Nonlinear time se... [35] Sobottka M., de Oliveira L.P.L. Periodic... [36] Fraser A.M., Swinney H.L. Independent co... [37] Bradley E., Kantz H. Nonlinear time-seri... [38] Abarbanel H. Analysis of observed chaoti... [39] Mayora-Cebollero C., Mayora-Cebollero A.... [40] Ayers D., Lau J., Amezcua J., Carrassi A... [41] Milly P.C.D., Wetherald R.T., Dunne K.A.... [42] Kangrang A., Pakoktom W., Nuannukul W., ... [43] Kratzert F., Klotz D., Brenner C., Schul... [44] Mosavi A., Ozturk P., Chau K., Flood pre... [45] Songsaengrit S., Kangrang, A. Dynamic ru...

Introduction

Rivers, as integral components of hydrological and climatic systems, play an indispensable role in providing fresh water, sustaining aquatic ecosystems, and supporting the socio-economic development of human communities [1]. However, surface flows often exhibit complex and nonlinear behavior, characterized by highly variable, irregular, and, in many cases, chaotic patterns [2]. Understanding the inherent features of river discharge time series, including the presence or absence of chaotic behavior, is a crucial step in the sustainable management of water resources and in forecasting the impacts of climate change on hydrological systems [3]. This understanding not only contributes to a better grasp of flow dynamics but also lays the foundation for designing more accurate predictive models and efficient management policies [4].

The significance of studying river flow behavior becomes even more pronounced as neglecting complex, nonlinear patterns can lead to the development of inefficient management programs, especially in scenarios where climate change and human activities exert increasing pressure on water resources [5]. In this regard, identifying chaotic patterns in discharge time series can help improve flow forecasting, flood risk management, and the formulation of adaptive policies in response to hydrological variability [2]. This need is particularly evident in regions with variable climates and fragile ecosystems, such as the watersheds in Iran.

Chaos theory provides a theoretical framework for analyzing nonlinear dynamical systems where, despite the presence of deterministic equations, long-term prediction becomes difficult due to extreme sensitivity to initial conditions [6,7]. In this theory, chaotic behavior is identified through the presence of a strange attractor in phase space, fractional correlation dimension, and positive Lyapunov exponent [8]. These characteristics indicate that seemingly random fluctuations within a system can result from deterministic but nonlinear dynamics [9,10]. In hydrology, such behavior often arises from the complex interactions between climatic factors such as precipitation and evaporation, topographic features of the watershed, and human interventions such as dam construction and land-use changes [7].

Several studies in the field of hydrology have confirmed the presence of chaotic behavior in river discharge time series. For example, Khatibi et al. [11] identified chaotic behavior at the Sogutluhan hydrometric station in Türkiye; Albostan & Önöz [1] reported similar findings in Turkish rivers; Zounemat-Kermani [12] observed chaos in the Daintree River of Australia; Ogunjo et al. [13] confirmed this behavior in the Niger River; Rezaie et al. [14] found similar results for the Sefidrood River in Iran; and Rolim & de Souza Filho [15] reported chaos in Brazilian river watersheds. These studies demonstrate that chaos theory tools, such as phase space reconstruction, correlation dimension analysis, and Lyapunov exponent estimation, are effective in identifying nonlinear dynamics of surface flows. Despite the growing global interest in applying chaos theory to hydrology, its implementation in Iranian watersheds remains limited, primarily due to challenges related to data continuity, quality, and the complexity of nonlinear analytical methods. This study aims to address this gap by applying chaos diagnostics to a rare, long-term, and high-quality streamflow dataset from the Gilvan Sub-Watershed, which provides an opportunity to explore the nonlinear dynamics of river systems in northwestern Iran more reliably.

The Gilvan Sub-Watershed, a tributary of the Qezel Ozan River and part of the Sefidrood Basin, offers an ideal case study due to the availability of consistent hydrological records (1963–2017), its distinctive snowmelt-driven regime, and its exposure to upstream human interventions. In particular, the basin's montane setting and strong seasonal variability in runoff contribute to nonlinear streamflow behavior, making it well-suited for chaos-based analysis. These features underline the novelty of applying chaos theory tools in this context, where short or discontinuous datasets have limited previous studies.

This study addresses several common limitations in chaos-based hydrological research by utilizing a continuous 54-year dataset from the Gilvan Station and applying rigorous tools such as phase space reconstruction, correlation dimension, and Lyapunov exponent analysis**.** These methodological strengths reinforce the reliability of the results and demonstrate the practical value of chaos theory in understanding hydrological complexity in snow-influenced, mountainous sub-watersheds like Gilvan, where traditional linear models often fall short.

The primary objective of this study is to investigate the chaotic behavior of the discharge time series from the Gilvan Sub-Watershed, a tributary of the Qezel Ozan River, using long-term data from the Gilvan station. Specifically, this research aims to:

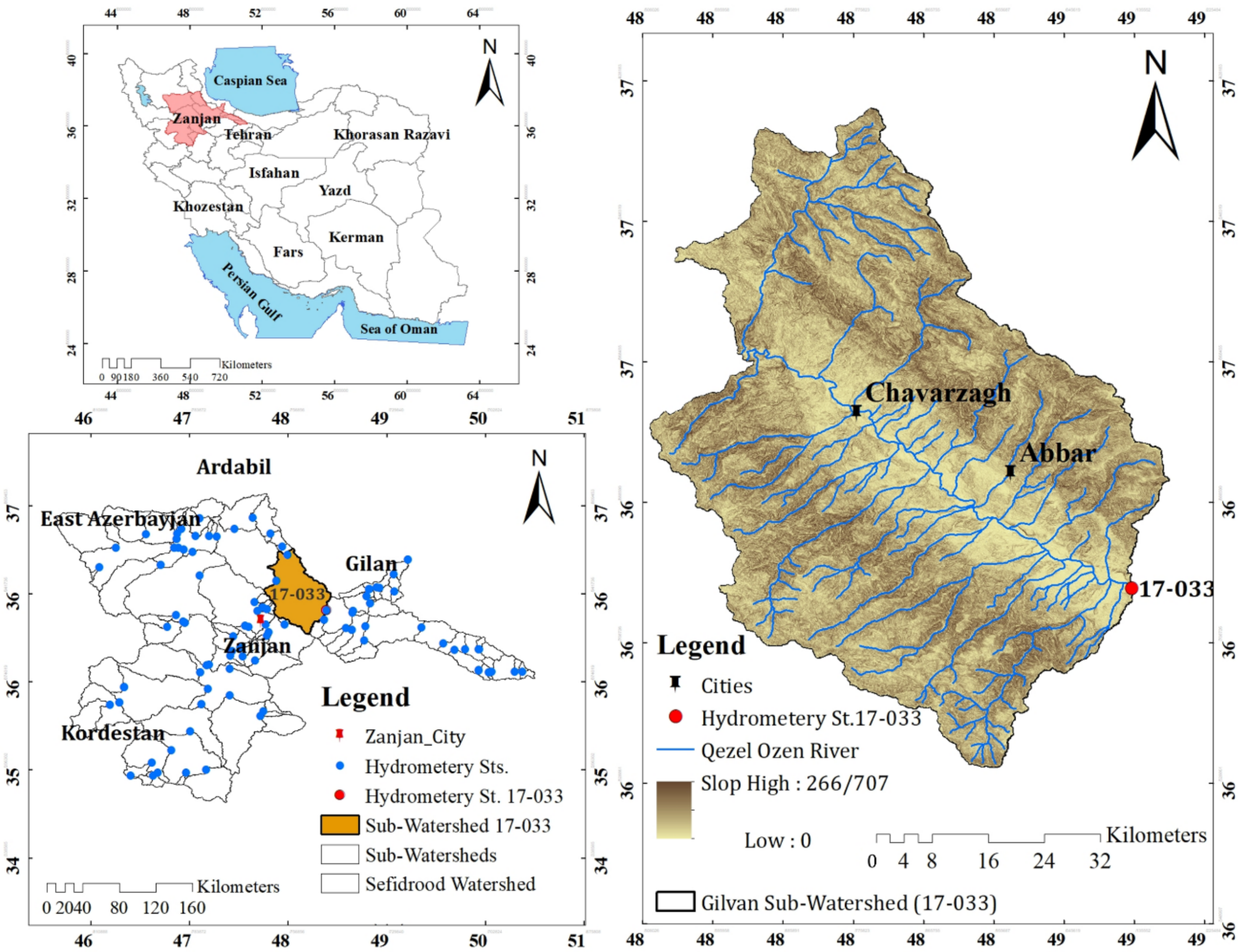

Figure 1) Location of the study area within the Sefidrood Watershed, highlighting the Gilvan Sub-Watershed, Zanjan Province, Iran (Code: 17-033).

The slope across the sub-watershed ranges from 0% to 266.7%, indicating considerable topographic variation.

(1) reconstruct the phase space of the river flow and identify the presence of a strange attractor, (2) determine key parameters such as optimal delay time and embedding dimension, (3) confirm the presence or absence of chaos by calculating the correlation dimension and largest Lyapunov exponent, and (4) provide insights for advanced modeling and optimal water resource management in the watershed.

Materials & Methods

Geographical Setting of the Study Area

This study focuses on the Gilvan Sub-Watershed, a key hydrological unit within the Sefidrood Watershed, located in the southern part of Zanjan Province, which offers a long-term and consistent daily streamflow record suitable for nonlinear and chaos analysis [16]. Covering an area characterized by varied topography, the Gilvan Sub-Watershed features elevations ranging from 300 m to over 3,000 m [17] and slopes varying from 0% to 266.7% (approximately 69°) in steep mountainous areas, as determined by ArcGIS slope analysis. It includes a partial contributing area of 29.90 km^2 and a total upstream drainage area of approximately 4988.32 km^2, with an average elevation of 1,514 m and a regional slope averaging around 20.5%. These physiographic characteristics, combined with seasonal precipitation patterns, drive nonlinear and potentially chaotic streamflow dynamics, making the sub-watershed an ideal candidate for chaos theory analysis [9]. Climatically, the area features a temperate, Mediterranean precipitation regime with winter-dominant rainfall and significant snowmelt, receiving approximately 300–800 mm annually [18]. Geologically, the watershed includes a mixture of tertiary volcanic and intrusive rocks, contributing to the spatial heterogeneity of runoff generation [19].

Hydrological data for this study were obtained from the Gilvan hydrometric station No. 17-033. Daily streamflow records from 1963 to 2017 (54 years) were used without temporal downsampling to preserve the full resolution of the nonlinear dynamics

This extended time series is particularly valuable for capturing the nonlinear dynamics and potential chaotic patterns in river discharge [11,14], as it encompasses a wide range of climatic and anthropogenic influences, including extreme events such as floods and droughts.

Figure 1 presents the geographic extent of the Sefidrood River Watershed in northwestern Iran and the location of the Gilvan Sub-Watershed within it. The map also shows the distribution of hydrometric stations, including station No. 17-033, and the slope variation (%) across the Gilvan Sub-Watershed.

Noise Detection in Hydrological Time Series

In nonlinear and chaotic system analysis, the presence of noise can significantly obscure the system's intrinsic properties [19]. Noise typically appears as random, unpredictable fluctuations in the data and may mask genuine chaotic patterns [20]. Given the high sensitivity of methods such as the Lyapunov exponent and correlation dimension to data quality, identifying and mitigating noise is a critical initial step.

Spectral analysis is a practical approach for detecting noise in time series [21]. In general, a noise-free time series displays a power spectrum with clear peaks at specific frequencies, indicating periodic or organized behavior. In contrast, noisy series—particularly those affected by white or colored noise—exhibit either a flat spectrum (white noise) or a spectrum with a smooth downward slope (e.g., Brownian noise) [22]. To further verify the presence of colored noise, the slope of the log–log plot of power versus frequency was examined: a slope near -2 suggests Brownian noise, while a slope around -1 indicates pink noise [23].

Fourier-based spectral analysis was used in this study to identify noise in the discharge time series before applying nonlinear methods. This method decomposes the time series into its frequency components, allowing for the detection of hidden patterns or anomalies as shown in Eq. (1) [24–26].

$$Z_t = a_0 + \sum_{i=1}^{m}\left[a_i \cos\left(2\pi f_i t\right) + b_i \sin\left(2\pi f_i t\right)\right] \quad \text{Eq. (1)}$$

In Eq. (1), Z_t represents the variable under analysis, and a_0, a_i, and b_i are the Fourier coefficients, which can be estimated using the least squares method. Once the Fourier coefficients are obtained, the periodogram can be computed. The periodogram can be represented in various forms, such as power versus frequency or variance versus frequency [24,25]. After calculating the periodogram, it can be smoothed to estimate the spectral density. The smoothed periodogram serves as an estimate of the population spectrum [24].

It should be noted that before performing spectral analysis, detrending the time series is essential, as trends can significantly affect the power spectrum [21,25]. Trends usually appear as low-frequency components with high power and can mask the effects of noise and chaotic dynamics. Detrending ensures that the spectral analysis focuses solely on the system's intrinsic fluctuations rather than long-term structural changes that lie outside the scope of chaotic dynamics. Therefore, in this study, before conducting spectral analysis, the trend component was estimated using a least squares regression model and subsequently removed from the original time series.

Phase Space Reconstruction

To reconstruct and visualize the phase space of the discharge time series from the Gilvan Sub-Watershed, the time delay embedding method was employed. This technique, based on Takens' Theorem [27], allows the hidden dynamics of a complex system to be reconstructed from a one-dimensional time series in a multidimensional phase space. The key parameters in this method are time delay and embedding dimension, which respectively define the optimal time interval between data points and the number of dimensions required to reveal the system's dynamics.

Time Delay

The estimation of the time delay (τ) for phase space reconstruction is typically done using two methods, autocorrelation or Average Mutual Information (AMI). The autocorrelation function primarily examines linear dependencies between data points, whereas the Average Mutual Information method can account for both linear and nonlinear dependencies. Therefore, when analyzing complex systems such as hydrological or climatic systems, which exhibit nonlinear and chaotic behavior, the AMI method may provide better performance. The Average Mutual Information method operates based on information theory and assesses the amount of shared information between a time series and its delayed version. In other words, this method indicates the probability that neighboring points, such as x(t) and x(t+τ), are statistically dependent. If P(x(t), x (t+τ)) is the probability distribution of the points and P(x(t))P(x (t+τ)) is their joint probability distribution, the Average Mutual Information is calculated as Eq. (2) [6].

$$AMI = \sum_{t=1}^{N-1} P(x(t),x(t+\tau)) \log \frac{P(x(t),x(t+\tau))}{P(x(t))P(x(t+\tau))} \quad \text{Eq. (2)}$$

In the AMI method, the first time delay at which the mutual information reaches a local minimum is typically considered the optimal time delay.

To ensure reproducibility and methodological clarity, the nonlinear analysis steps were implemented using custom MATLAB scripts written by the authors.

The computation of Average Mutual Information (AMI) followed the method described by Fraser and Swinney [35], with probability density estimation performed using uniform binning and the Freedman–Diaconis rule for bin width selection.

For the False Nearest Neighbors (FNN) method, the Euclidean distances between reconstructed vectors were calculated, and the proportion of false neighbors was tracked across dimensions. A threshold of 10% was used to identify the optimal embedding dimension.

The correlation dimension was estimated using the Grassberger–Procaccia algorithm, and the largest Lyapunov exponent was calculated using the Rosenstein method, focusing on short-term trajectory divergence. All analyses were conducted on the monthly discharge dataset (1963–2017) from the Gilvan station (Code: 17-033) using MATLAB R2022a. Although the code is not publicly available due to its proprietary nature, key implementation details can be provided upon request for academic purposes.

Embedding Dimension

To determine a suitable embedding dimension for reconstructing the phase space of the discharge time series, the False Nearest Neighbors (FNN) method was employed. This method evaluates the dimension in which discontinuities or inconsistencies in phase space trajectories are minimized or eliminated. In other words, if the phase space is embedded in an appropriate dimension, the trajectories do not intersect, and the discontinuities caused by projecting the phase space into too low a dimension disappear. In nonlinear dynamical systems such as river flow—which may exhibit chaotic or near-chaotic behavior—selecting an appropriate embedding dimension is essential to prevent trajectory crossings and to reconstruct the system's dynamics accurately.

In the False Nearest Neighbors (FNN) method, the first step involves constructing delay vectors using the optimal time delay and a trial embedding dimension mmm. These vectors are generated from the time series to represent the system's states in the reconstructed phase space. The delay vector $Y_i(t)$ is defined as Eq. (3) [28].

$$Y_i(t) = \left[Y(t), Y(t-\tau), Y(t-2\tau), \ldots, Y(t-(m-1)\tau)\right]^T \quad \text{Eq. (3)}$$

The above Eq. illustrates that two key factors determine the construction of delay vectors, including the number of components in each vector, which corresponds to the embedding dimension (m), and the time interval between successive components, which is the time delay (τ). Once the delay vectors are constructed, the r^{th} nearest neighbor of each delay vector $Y_r^{NN}(t)$ is identified as Eq. (4) [28].

$$Y_r^{NN}(t) = \left[Y(t_r), Y(t_r-\tau), Y(t_r-2\tau), \ldots, Y(t_r-(m-1)\tau)\right]^T \quad \text{Eq. (4)}$$

where t_r denotes the time index of the r^{th} nearest neighbor to $Y_r^{NN}(t)$ in the m-dimensional phase space. The distance between two neighboring delay vectors is calculated using the Euclidean norm, as Eq. (5) [28].

$$R_m^r = \sum_{i=0}^{m-1}\left[Y(t-i\tau) - Y(t_r-i\tau)\right]^2 \quad \text{Eq. (5)}$$

If the vector $Y_r(t)$ is a true neighbor of $Y(t)$, this closeness reflects the actual dynamics of the system. However, if this proximity results merely from projecting a higher-dimensional phase space into a lower dimension, then upon increasing the embedding dimension from m to m+1, this neighbor will no longer remain close. Such a neighbor is referred to as a false nearest neighbor.

When the embedding dimension is increased from m to m+1, the newly added components to the delay vectors $Y_r(t)$ and $Y(t)$ are and respectively. Consequently, the Euclidean distance between the two vectors in the (m+1)-dimensional phase space is calculated as Eq. (6) [28].

$$R_{m+1}^2 = \sum_{i=0}^{m}[Y(t-i\tau)-Y(t_r-i\tau)]^2 = R_m^2 + [Y(t-m\tau)-Y(t_r-m\tau)]^2 \quad \text{Eq. (6)}$$

The relative added distance, compared to the distance between the two delay vectors in the original m-dimensional space, is computed as Eq. (7) [28].

$$\sqrt{\frac{R_{m+1}^2 - R_m^2}{R_m^2}} = \frac{\left|Y(t-m\tau)-Y(t_r-m\tau)\right|}{R_m} \quad \text{Eq. (7)}$$

If the value obtained from the equation above exceeds a predefined threshold, the neighbor is classified as a false nearest neighbor. Based on previous research, it is recommended that this threshold be set between 10 and 15 [29].

This procedure is repeated for delay vectors constructed with progressively increasing embedding dimensions until the percentage of false nearest neighbors approaches zero or becomes negligibly small. The embedding dimension at which this occurs is then selected as the appropriate dimension for phase space reconstruction.

This method ensures that the phase space is reconstructed in such a way that phase trajectories do not intersect, and the nonlinear dynamic structure of the system is accurately revealed. Selecting an appropriate embedding dimension is essential for subsequent analyses, such as the computation of Lyapunov exponents.

Construction of Delay Vectors and Phase Space Plotting

In the next step, using the previously determined optimal time delay and embedding dimension, delay vectors are constructed in phase space based on Eq. (3). However, for visualization purposes, typically only two or three components of these vectors are plotted in a two- or three-dimensional space, although the actual system dynamics exist in a higher-dimensional space.

In general, plotting the phase space and identifying strange attractors facilitates the recognition of chaotic behaviors. In systems such as river flow dynamics, such behavior may indicate sensitivity to initial conditions, nonlinear responses, and the influence of climatic and environmental variables [30].

Chaos Analysis

Correlation Dimension

The correlation dimension is one of the most widely used and fundamental metrics for identifying and characterizing nonlinear dynamical systems, particularly chaotic systems. It helps assess the geometric and structural complexity of strange attractors in phase space and is commonly employed to distinguish between random, deterministic, and chaotic processes.

In this study, the correlation dimension is estimated using the correlation integral. The underlying assumption of this method is that purely random processes exhibit an infinite (continuous) dimension, while chaotic processes possess a finite, often fractal dimension. The approach involves constructing a hypersphere around a reference point in the phase space and gradually increasing its radius until it encompasses all points in the reconstructed attractor.

The correlation integral C(r), for an m-dimensional phase space, is defined as Eq.(8) [31].

$$C(r) = \lim_{N\to\infty} \frac{2}{N(N-1)} \sum_{i,j} H(r-\left|Y_i - Y_j\right|) \quad \text{Eq. (8)}$$

where H is a Heaviside step function, defined as Eq. (9):

$$H(u) = \begin{cases} 1 & \text{if} \quad u \geq 0 \\ 0 & \text{if} \quad u < 0 \end{cases} \quad \text{Eq. (9)}$$

In the above expressions, r represents the radius of the hypersphere centered at Y_i or Y_j , and N is the total number of points in the phase space. For positive values of r, the correlation integral is related to r by the following expression (Eq. (10)).

$$C(r) \underset{r\to 0,\, N\to\infty}{\approx} a r^{D_2} \qquad \text{Eq. (10)}$$

where a is a constant coefficient, and D_2 is the correlation exponent. The correlation dimension D_2 is calculated using Eq. (11).

$$D_2 = \lim_{r\to 0,\, N\to\infty} \frac{\log C(r)}{\log(r)} \qquad \text{Eq. (11)}$$

In practice, C(r) is plotted against log r, and the slope of the linear portion of the resulting graph is estimated using the least squares method for various embedding dimensions. Then, by plotting D_2 versus the embedding dimension, the nature of the underlying process can be determined. If D_2 increases continuously without saturation as the embedding dimension increases, the process is random. If the graph saturates, it suggests a deterministic process. Furthermore, if the saturated value of D_2 is non-integer, the system is considered chaotic.

Lyapunov Exponent

The Lyapunov exponent is a fundamental indicator used to identify chaotic behavior in dynamical systems, including river discharge time series. This exponent quantifies the rate of divergence between neighboring trajectories in the reconstructed phase space. In chaotic systems, the presence of at least one positive Lyapunov exponent signifies sensitivity to initial conditions and the nonlinear deterministic nature of the system [30].

The Lyapunov spectrum can be computed from the reconstructed attractor. While many existing methods for calculating these exponents are mathematically intensive and complex, the algorithm proposed by Rosenstein provides a relatively straightforward approach to estimate the largest Lyapunov exponent (λ_{max}) [6].

To apply the Rosenstein method, a reference point Y_i is selected in the phase space, and the average distance of all neighboring points s_n, which lie within a specific radius r of the reference point, is computed. This process is repeated for N points and is referred to as the stretching factor (Eq. (12)) [32].

$$S = \frac{1}{N}\sum_{n_0=1}^{N} \ln\left(\frac{1}{\left|U(s_{n_0})\right|}\sum\left|s_{n_0} - s_n\right|\right) \qquad \text{Eq. (12)}$$

In Eq. (12), M represents the number of neighboring points identified around each reference point Y_i. By plotting the stretching factor S(N) against the number of time steps N, or equivalently against time t=NΔt, a curve is obtained whose linear region's slope provides an approximation of the largest Lyapunov exponent. If the estimated λ_{max} is positive, it serves as strong evidence that the system exhibits chaotic behavior.

Findings

Streamflow Characteristics and Trend Analysis

Figure 2 illustrates the monthly time series of the discharge from the Gilvan Sub-Watershed from 1963 to 2017. During this period, the mean discharge was approximately 89.7 $m^3.s^{-1}$. The maximum recorded discharge occurred in April 1968, reaching a peak value of 1206.3 $m^3.s^{-1}$.

Trend analysis of the streamflow data was conducted using linear regression, which revealed a statistically significant decreasing trend at the 99% confidence level (p-value = 0.000). The regression model y=141.4−0.16t suggests that, on average, the monthly discharge has decreased by approximately 0.16 $m^3.s^{-1}month^{-1}$ over the study period. This decline likely reflects the combined impacts of climate variability, reduced precipitation, snowmelt changes, upstream water withdrawals, and land-use alterations. From a dynamical perspective, the long-term downward trend indicates evolving boundary conditions that may influence the geometry of the reconstructed attractor and the intensity of chaotic behavior. While the system still exhibits key features of deterministic chaos, such as sensitivity to initial conditions, the reduced variability may limit predictability horizons. These findings highlight the necessity of adopting adaptive, nonlinear models that account for nonstationarity in river systems, particularly for long-term water management and environmental flow assessment.

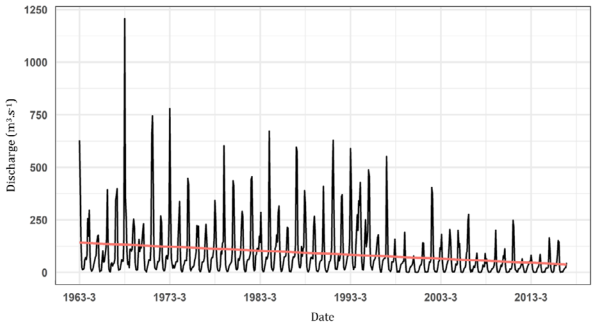

Figure 2) Monthly time series of river discharge over the period 1963–2017 from the Gilvan Sub-Watershed, Zanjan Province, Iran.

Noise Assessment Test

To evaluate the presence or absence of noise in the time series, spectral analysis was employed. Given that trends can influence the outcome of spectral analysis, the original monthly discharge series from the Gilvan Sub-Watershed was first detrended. The detrended time series is illustrated in Figure 3 (A), while the power spectrum of the detrended data is shown in Figure 3 (B).

The power spectrum reveals three dominant peaks at frequencies of 0.0833, 0.1667, and 0.25, corresponding to return periods of 12 months, 6 months, and 4 months, respectively. These peaks confirm the presence of seasonal patterns and indicate a strong cyclical structure within the time series. Such periodic components are typically associated with natural hydrological processes, including seasonal rainfall and snowmelt dynamics.

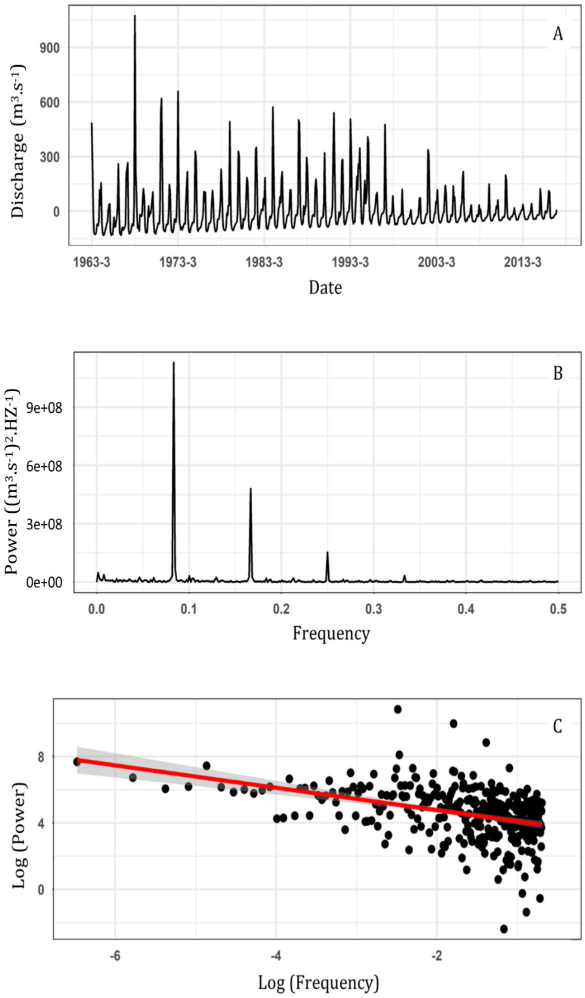

Figure 3) (A) Detrended monthly streamflow time series; (B) Power spectral density of the detrended series; (C) Log–log plot of power spectral density versus frequency for noise characterization from the Gilvan Sub-Watershed, Zanjan Province, Iran.

The presence of distinct peaks and significant variations in power across different frequencies suggests that the time series does not follow a white noise process, which is characterized by a flat, featureless power spectrum [30]. Furthermore, the noticeable decline in power at higher frequencies also implies the absence of colored noise such as Brownian noise ($1.f^{-2}$) or pink noise ($1.f^{-1}$) [33]. To further verify this, the log–log slope of the power spectrum was computed and is presented in Figure 3 (C). The estimated slope is −0.6, which is significantly lower in magnitude than what is typically expected for pink noise (−1) or Brownian noise (−2). This supports the conclusion that the time series does not contain meaningful colored noise either. Therefore, the data exhibits a structured, predictable pattern, making it well-suited for further nonlinear and chaos-based analyses.

Phase Space Reconstruction

Time Delay Selection

To determine the optimal time delay for phase space reconstruction, the Average Mutual Information (AMI) method was employed. The results are illustrated in Figure 4, where the AMI function reaches its first local minimum at a delay of 2. At this point, the mutual information between the current and lagged values of the time series declines significantly, approaching zero. This behavior suggests that a delay of 2 offers a balance between redundancy and statistical independence of the delayed components. Hence, a time delay of 2 was selected as the optimal value for reconstructing the phase space of the discharge time series. This choice ensures the unfolding of the system's hidden nonlinear dynamics in a manner that avoids over-correlation and allows for the revelation of potential chaotic behavior embedded in the hydrological system [34].

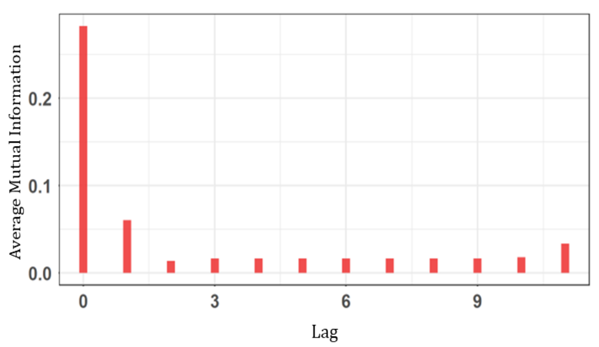

Figure 4) Average Mutual Information (AMI) of the monthly discharge time series from the Gilvan Sub-Watershed, Zanjan Province, Iran

Embedding Dimension

To determine the appropriate embedding dimension, the False Nearest Neighbors (FNN) method was applied. As illustrated in Figure 5, the percentage of false neighbors decreases as the embedding dimension increases, and the slope of the curve approaches zero at dimension 6. Beyond this point, the changes become negligible, and the percentage of false neighbors remains nearly constant. This pattern indicates that, at dimension 6, the phase space has been sufficiently unfolded, resulting in an adequate reconstruction of the system's dynamics.

In lower dimensions (less than 6), the projection of the time series into a reduced-dimensional space leads to the emergence of false neighbors due to an improper mapping of the system’s nonlinear dynamics [29]. Conversely, increasing the dimension beyond six yields minimal improvements and may even introduce unnecessary noise. Therefore, selecting six as the optimal embedding dimension ensures that the reconstructed phase space accurately captures the system's true dynamics while avoiding overfitting and the incorporation of spurious data, which could arise from an excessively high embedding dimension.

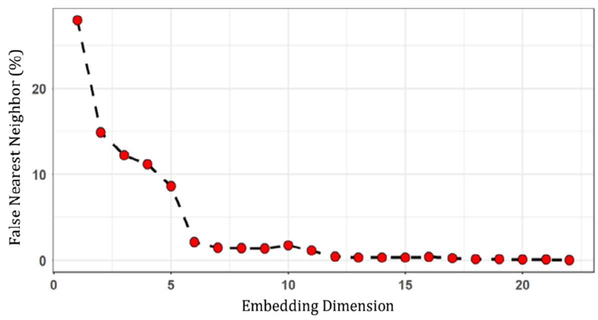

Figure 5) False Nearest Neighbors (FNN) plot for determining the optimal embedding dimension.

Phase Space Reconstruction

Figure 6 presents the phase space reconstruction of the river discharge in both two-dimensional and three-dimensional forms, using a time delay of two months. The observed patterns in the reconstructed phase space indicate a complex and nonlinear structure. The points are not randomly scattered; instead, they cluster in specific regions of the phase space, suggesting the presence of a strange attractor.

Moreover, the sensitivity to initial conditions is evident; minor differences in the initial values of the time series result in significantly divergent phase trajectories. Additionally, the phase trajectories do not follow a fixed line or repetitive path; instead, they display intricate and recurring patterns that revolve around a structured shape. These features include structured yet non-repetitive trajectories, sensitivity to initial conditions, and the presence of an apparent attractor, which are hallmark characteristics of chaotic systems [35]. Consequently, these results imply that the discharge of the river may exhibit chaotic or near-chaotic behavior, which is consistent with the dynamics of many natural hydrological systems [36].

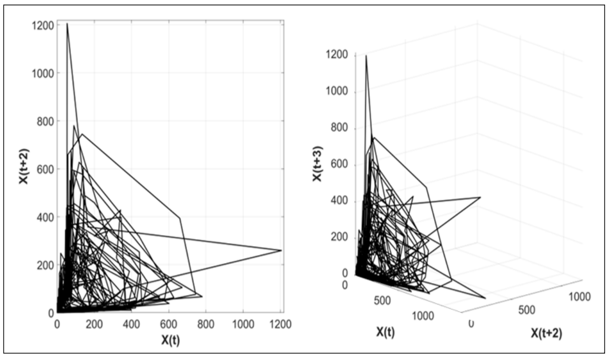

Figure 6) Reconstructed phase space of the discharge time series from the Gilvan Sub-Watershed, Zanjan Province, Iran, using optimal parameters (time delay τ = 2 months, embedding dimension m = 6).
(Left): 2D projection of the attractor in the plane X(t) vs. X(t+2). (Right): 3D phase space plot showing trajectories in X(t), X(t+2), X(t+3), where signs of trajectory divergence and attractor folding are observable. These features indicate sensitivity to initial conditions and the presence of a low-dimensional chaotic attractor, despite the projection from the full 6D embedding space.

Quantitative Assessment of Chaos
Estimation of the Correlation Dimension

Figure 7 illustrates the log-log plot of the correlation integral versus radius for increasing embedding dimensions, applied to the river discharge time series. The figure displays three distinct regions: the sparsity region (small values of log(Cr)), the saturation region (large values of log(Cr)), and the scaling region (the intermediate portion of log(Cr)).

Part B of the figure presents the estimated correlation dimension (D_2) as a function of increasing embedding dimension. The results indicate that for lower embedding dimensions, the correlation dimension increases gradually, eventually reaching a saturation value of approximately 2.3. This saturation implies that the attractor's geometry is fully unfolded within this dimensional setting and does not gain additional complexity with further embedding.

A non-integer correlation dimension, particularly one that stabilizes, is a strong indication of a strange attractor and, consequently, chaotic behavior in the river discharge dynamics. These findings are consistent with established methodologies for detecting deterministic chaos in nonlinear hydrological systems [35].

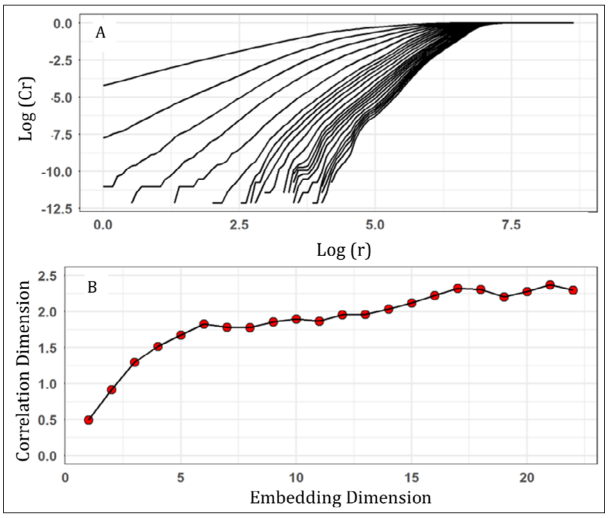

Figure 7) (A) Correlation integral curves illustrating how point clustering in phase space changes with radius and embedding dimension. (B) Correlation dimension versus embedding dimension, showing convergence around 2.3, which suggests a chaotic dynamic structure in the discharge time series from the Gilvan Sub-Watershed, Zanjan Province, Iran.

Largest Lyapunov Exponent

The estimated Lyapunov exponents for the river discharge time series are presented in Figure 8. Initially, the Lyapunov exponents increase rapidly, indicating a swift divergence of nearby trajectories in phase space. Subsequently, the curve enters a linear phase and eventually saturates, stabilizing at a specific value. The slope of the linear region is taken as an estimate of the largest Lyapunov exponent, which was found to be +0.08.

The positive value of the largest Lyapunov exponent strongly suggests that the discharge dynamics of the river exhibit chaotic behavior. This implies that even small differences in initial river flow conditions may lead to significantly different future outcomes, highlighting the inherent unpredictability and complexity in the river's hydrological dynamics.

Recent studies have explored advanced methods for estimating Lyapunov exponents from time series data. For instance, Mayora-Cebollero et al. [37] employed deep learning techniques to approximate the full Lyapunov exponent spectrum from single-variable time series, demonstrating the potential of machine learning in chaotic system analysis. Additionally, Ayers et al. [38] utilized supervised machine learning to estimate local Lyapunov exponents, offering a computationally efficient alternative to traditional methods.

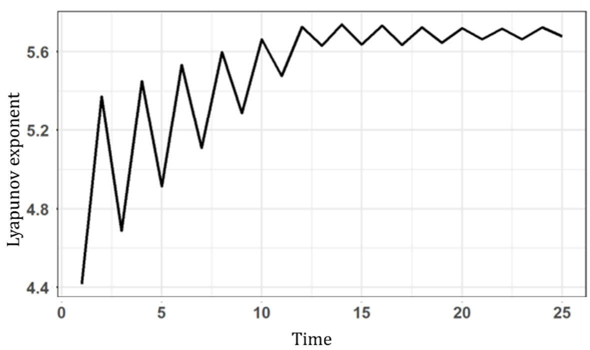

Figure 8) Lyapunov exponent for the time series of discharge from the Gilvan Sub-Watershed, Zanjan Province, Iran.

Table 1 summarizes the key parameters derived from the nonlinear analysis, providing a quick reference to support the interpretation of chaotic behavior in the river discharge series from the Gilvan Sub-Watershed.

Discussion

The findings of this study provide compelling evidence that the monthly discharge in Gilvan Sub-Watershed exhibits characteristics of a deterministic chaotic system. Through the use of chaos theory—specifically Average Mutual Information (AMI), False Nearest Neighbors (FNN), correlation dimension, and Lyapunov exponent analysis—the underlying nonlinear dynamics of the system were revealed. The optimal time delay (τ = 2 months) and embedding dimension (m = 6) allowed for meaningful phase space reconstruction. The calculated correlation dimension (D_2 = 2.3) indicates a low-dimensional attractor, while the positive largest Lyapunov exponent (λ_max = 0.08) confirms the system's sensitivity to initial conditions, a hallmark of chaos.

Given that our dataset consists of daily or coarser temporal resolution data, the presence of high-frequency noise is expected to be minimal. Moreover, spectral analysis indicated no significant trends or noise components that would necessitate the application of noise-reduction techniques such as Singular Spectrum Analysis (SSA). However, it is essential to acknowledge that chaos theory tools inherently have limitations in fully distinguishing deterministic chaos from stochastic influences. This limitation should be considered when interpreting the results.

The Gilvan Sub-Watershed's slightly lower correlation dimension suggests that its attractor is less geometrically intricate than that of the Niger River [13]. This could be attributed to its mountainous topography, snowmelt-dominated runoff regime, and localized human activities such as upstream

Table 1) Summary of key parameters used in chaos analysis of the discharge time series from the Gilvan Sub-Watershed, Zanjan Province, Iran.

Parameter	Value	Method Used	Notes
Time Series Length	1963–2017	-	55 Years of Monthly Data (No Missing Values)
Time Delay (τ)	2 Months	Average Mutual Information (AMI)	First Minimum of AMI
Embedding Dimension (m)	6	False Nearest Neighbors (FNN)	Chosen to Minimize False Neighbors
Correlation Dimension (D_2)	2.3	Grassberger–Procaccia Algorithm	Indicates Low-Dimensional Attractor
Largest Lyapunov Exponent (λ_{max})	0.08	Rosenstein Method	Positive Value Confirms Deterministic Chaos
Trend in Discharge	−0.16 $m^3 \cdot s^{-1} month^{-1}$	Linear Regression	Statistically Significant at 99% Confidence
Spectral Analysis Outcome	No Significant Noise	Power Spectrum Analysis	No Need for Noise Reduction (e.g., SSA)

water withdrawals and land-use changes. Unlike tropical rivers that often exhibit high and continuous precipitation [14], the Gilvan sub-watershed experiences marked seasonal variation in streamflow driven by snow accumulation and melt. This seasonal intermittency may contribute to more structured but still chaotic hydrological patterns.

Furthermore, the influence of large-scale climate oscillations—particularly the El Niño–Southern Oscillation (ENSO)—has been shown to enhance nonlinear responses in river discharge. Studies such as Zhao et al. [5] have illustrated that ENSO-driven rainfall anomalies can amplify chaotic behavior in streamflow, especially in watersheds where precipitation variability is high. The Gilvan Sub-Watershed, located in a climate transition zone, is highly responsive to such interannual variability. This makes it more susceptible to dynamic shifts in discharge behavior, with small perturbations in precipitation or snowmelt potentially resulting in vastly different hydrological responses.

The presence of chaotic dynamics in river systems is not uniform and is highly dependent on the interplay of climatic, topographic, and anthropogenic factors. For instance, rivers in tropical humid climates often exhibit stronger seasonal cycles with lower chaotic intensity due to more consistent rainfall patterns. In contrast, rivers in snowmelt- or rainfall-dominated temperate, Mediterranean watersheds, such as the Gilvan Sub-Watershed, tend to show higher susceptibility to nonlinear behaviors due to the delayed and intermittent nature of runoff processes. This observation aligns with findings by Sivakumar [9], who emphasized that chaos is more prominent in watersheds where episodic events and irregular climatic forcing govern runoff.

From a climatological perspective, the observed chaotic behavior may be further exacerbated under future climate change scenarios. Increasing temperature trends, changes in snowpack dynamics, altered timing and magnitude of precipitation events, and the frequency of extreme hydrological events (e.g., droughts and floods) are all likely to intensify the complexity of river discharge patterns. Milly et al. [39] have argued that traditional assumptions of stationarity in hydrology are no longer valid under nonstationary climate conditions. In this context, deterministic chaos offers a powerful conceptual framework to understand how hydrological systems may evolve in response to changing boundary conditions.

The implications for water resources management are substantial. The presence of chaos implies a limited forecasting horizon beyond which the reliability of predictions declines significantly. This presents serious challenges for long-term planning in water supply, irrigation scheduling, dam operation, and flood risk reduction. The inadequacy of conventional linear time series models—such as ARIMA or regression-based methods—in capturing such dynamics underscores the need for more robust, nonlinear forecasting tools. Recent studies have demonstrated the successful use of chaos-informed nonlinear models such as Long Short-Term Memory (LSTM) networks and Artificial Neural Networks (ANNs) in forecasting streamflow in chaotic systems. For instance, Kratzert et al. [40] utilized LSTM networks to forecast river discharge and showed significant improvement in accuracy compared to classical models. Similarly, Mosavi et al. [41] reviewed a range of ANN applications and emphasized their effectiveness in hydrological prediction under chaotic and uncertain conditions.

From a policy and management perspective, dynamic dam operation protocols based on real-time inflow anomaly detection have proven effective in systems influenced by chaotic hydrology. Songsaengrit et al. [42] demonstrated how adaptive reservoir operation could mitigate flood risk using such data-driven strategies. In another case, Kangrang et al. [43] proposed climate-informed reservoir rule curves that respond to ENSO forecasts and nonlinear system indicators. These examples support the integration of chaos-based diagnostics with adaptive infrastructure and real-time decision support systems. Additionally, given its upstream location, the Gilvan Sub-Watershed contributes seasonally significant inflows to the Sefidrood Dam, especially during the snowmelt period. These inflows are sensitive to both climatic and anthropogenic factors, making the sub-basin's discharge behavior directly relevant to downstream reservoir operations. As a result, the nonlinear and potentially chaotic nature of flow in this sub-basin could influence dam management strategies, especially under changing climate and land-use scenarios.

Recent advances in machine learning and hybrid modeling techniques offer promising avenues to complement chaos-based diagnostics. For example, artificial neural networks (ANNs), support vector machines (SVMs), and long short-term memory (LSTM) networks have demonstrated superior performance in forecasting nonlinear time series when trained with appropriate climatic and hydrological inputs. Integrating these data-driven models with chaos theory indicators can help extend the predictability window and improve real-time decision-making, especially in data-limited or uncertainty-prone environments.

Furthermore, from a systems management perspective, the recognition of chaotic behavior necessitates the design of adaptive, flexible infrastructure and management strategies. Multipurpose dams with dynamic release protocols, groundwater recharge systems, and integrated watershed management plans can enhance system resilience. Attention must also be given to preserving ecological flows and maintaining groundwater sustainability, which are often compromised in overly engineered and non-adaptive systems.

In summary, the application of chaos theory to the Gilvan Sub-Watershed has not only confirmed the system's nonlinear and sensitive behavior but has also aligned with a growing body of international research highlighting the ubiquity of chaos in river systems. The study contributes to a deeper theoretical understanding of hydrological complexity while offering practical insights for adaptive water management in the context of climate variability and change. Furthermore, as discussed earlier, anthropogenic interventions—particularly dam operations and upstream water abstractions—can interact with the nonlinear dynamics of river discharge. These actions may either amplify or dampen chaotic responses by modifying the timing, magnitude, and variability of streamflow, thereby influencing the system's sensitivity to initial conditions.

Conclusion

This study confirmed that the streamflow of the Gilvan Sub-Watershed is deterministic chaos, as suggested by a positive largest Lyapunov exponent ($\lambda\_max = 0.08$) and a finite correlation dimension ($D_2 = 2.3$). These parameters indicate the initial condition sensitivity of the system and the presence of low-dimensional chaotic dynamics.

Utilization of the phase space reconstruction techniques, in conjunction with AMI and FNN as a means of optimal parameter choice, provided a powerful analytical tool for characterizing the nonlinear dynamics of the discharge time series. The consequences of these findings are particularly far-reaching for mountainous, snowmelt-dominated sub-watersheds' water resource management. The presence of chaos indicates a limited prediction horizon, which compounds the difficulty of long-term flood control forecasting, reservoir design, and water supply reliability. The shortcomings of the common linear time series models emphasize the value of increased application of adaptive, nonlinear modeling techniques. While the study neither seeks to generalize results beyond the Gilvan Sub-Watershed nor seeks to make a necessarily unlimited generalizability claim, it does provide an educational case example of the promise of chaos theory in Iranian river environments. With continuous, long-term hydrological data being so unusually available in the nation, this research acts to complete a gap in the application of nonlinear methods to Iranian hydrology. Subsequent studies may capitalize on these findings through the integration of climate indices (e.g., ENSO), analysis of land-use change, and development of hybrid models for improving streamflow forecasting under uncertainty.

Acknowledgements

The authors would like to express their sincere appreciation to the National Office of Water Data and Information (Tamab) for providing the necessary hydrological data that made this research possible. This article is part of the results of a national research project entitled "Investigation of Temporal Changes and Trends of Low Flows in Major Watersheds of Iran," approved under the project code 01-29-29-045-00037-000888, and supported by the Agricultural Research, Education and Extension Organization (AREEO) – Soil and Water Conservation Research Institute.

Ethical Permission: The authors certify that this manuscript is original and that any use of others' work or words has been appropriately cited.

Authors' Contributions: All the authors of this article have cooperated in obtaining the data, analyzing the results, and compiling the article.

Funding Support: This article is part of the results of a national research project supported by the Agricultural Research, Education, and Extension Organization (AREEO) – Soil and Water Conservation Research Institute.

Conflict of Interests: The authors have no conflicts of interest to express consideration for the publication of this paper. They confirmed that co-authors have consented to and are fully aware of the submission.

References:

1. Albostan A., Önöz B. Implementation of chaotic analysis on river discharge time series. Energ. Pow. Eng. 2015; 7(1):81–92.
2. Mihailović D.T., Malinović-Milićević S., Han J., Singh V.P. Complexity and chaotic behavior of the US Rivers and estimation of their prediction horizon. J. Hydrol. 2023; 622:129730.
3. Baggaley N.J., Langan S.J., Futter M.N., Potts J.M., Dunn S.M. Long-term trends in hydro-climatology of a major Scottish mountain river. Sci. Total Environ. 2009; 407:4633–4641.
4. Martínez J.H., Lehnertz K., Rubido N. Introduction to focus issue: Data-driven models and analysis of complex systems. CHAOS 2025; 35.
5. Zhao Y., Zhu T., Zhou Z., Cai H., Cao Z. Detecting nonlinear information about drought propagation time and rate with nonlinear dynamic system and chaos theory. J. Hydrol. 2023; 623:129810.
6. Baker G.L., Gollub J.P. Chaotic dynamics: an introduction. Cambridge Univ. Press, 1996.
7. Cunico I., Bertoldi W., Caponi F., Dijkstra H.A., Siviglia A. River ecomorphodynamic models exhibit features of nonlinear dynamics and chaos. Geophys. Res. Lett. 2024; 51(11):e2023GL107951.
8. Li T., Lan T., Zhang H., Sun J., Xu C.-Y., Chen Y.D. Identifying the possible driving mechanisms in precipitation-runoff relationships with nonstationary and nonlinear theory approaches. J. Hydrol. 2024; 639:131535.
9. Sivakumar B. Chaos theory in hydrology: important issues and interpretations. J. Hydrol. 2000;227(1):1–20.
10. Ghorbani M.A., Kisi O., Aalinezhad M. A probe into the chaotic nature of daily streamflow time series by correlation dimension and largest Lyapunov methods. Appl. Math Model. 2010; 34:4050–4057.
11. Khatibi R., Sivakumar B., Ghorbani M.A., Kisi O., Koçak K., Zadeh D.F. Investigating chaos in river stage and discharge time series. J. Hydrol. 2012; 414(1):108–117.
12. Zounemat-Kermani M. Investigating chaos and nonlinear forecasting in short-term and mid-term river discharge. Water Resour. Manag. 2016; 30(5):1851–1865.
13. Ogunjo S., Olusola A., Fuwape I., Durowoju O. Temporal variation in deterministic chaos: the influence of Kainji dam on downstream stations along lower Niger River. Arab J. Geosci. 2022; 15(3):237.
14. Rezaie H., Garebaghi P., Khani Temeliyeh Z., Mirabbasi-Najafabadi R. Monthly flow analysis of Sefidrood River using chaos theory. Water Soil Manage. Model. 2022; 2(1):27–41.
15. Rolim L.Z.R., de Souza Filho F.A. Exploring spatiotemporal chaos in hydrological data: evidence from Ceará, Brazil. Stoch. Env. Res. Risk Assess. 2023;37(11):4513–4537.
16. Kavian A., Dodangeh S., Abdollahi Z. Annual suspended sediment concentration frequency analysis in Sefidroud Watershed, Iran. Model Earth Syst. Environ. 2016; 2(1):48.
17. Avarand Y., Janatrostami S., Ashrafzadeh A., Pirmoradian N. Developing fuzzy multi-objective planning model for agricultural water management in areas outside the Sefidrood irrigation and drainage network by determining effective precipitation. Iran J. Soil Water Res. 2023; 53(8):1901-1920..
18. Najafi M.S., Alizadeh O. Climate zones in Iran. Meteorol. Appl. 2023;30(5):1–10.
19. Zareian M.J., Seraj Ebrahimi R., Dehban H. Investigating the impact of climate change on extreme temperature and precipitation in the Sefidrood Watershed based on CMIP6 Models. JWSS 2024; 28(3):53–71.
20. Ghorbani A., Moameri M., Dadjou F., Seyedi Kaleybar S.A., Pournemati A., Asghari S. Determinization of environmental factors effects on plants production in QezelOzan-Kosar rangelands, Ardabil Province. ECOPERSIA 2020; 8(1):47–56.
21. Benmebarek S., Chettih M. Chaotic analysis of daily runoff time series using dynamic, metric, and topological approaches. ACTA Geophys. 2024; 72(4):2633–2651..
22. Kostelich E.J., Schreiber T. Noise reduction in chaotic time-series data: A survey of common methods. Phys. Rev. E. 1993; 48(3):1752.
23. Priestley M.B. The spectral analysis of time series. Oxford Univ Press; 1982.
24. Brockwell P.J., Davis R.A. Introduction to time series and forecasting. Springer; 2016.
25. Bloomfield, P. Fourier analysis of time series: an introduction. Wiley; 1976.
26. Asakereh H. Power spectrum analysis of the time series of Tabriz annual temperature. Geogr. Res.

2009; 24(3):33–50.
27. Cryer J.D. Chan K.S. Time series analysis. Springer; 2008.
28. Lin H. Nonlinear dynamic Process of fluvial process based on theories of chaos and dissipative structure. Preprint arXiv:250301593. 2025.
29. Takens F. Detecting strange attractors in turbulence. In: Rand D.A., Young L.S., editors. Dynamical Systems and Turbulence, Warwick 1980. Springer; 2006; 81-366.
30. Pari Zangeneh M., Ataei M., Moallem P. Phase space reconstruction of chaotic time series using an intelligent method. J. Electr. Eng. Dept., Trans. Electr. Technol. (Electron. Power). 2009; 1(2): 3-10.
31. Kennel M.B., Brown R., Abarbanel H.D.I. Determining embedding dimension for phase-space reconstruction using a geometrical construction. Phys. Rev. A. 1992; 45(6):3403.
32. Vallejo J.C., Sanjuan M.A.F. Predictability of chaotic dynamics. Springer; 2017.
33. Elshorbagy A., Simonovic S.P., Panu U.S. Noise reduction in chaotic hydrologic time series: facts and doubts. J. Hydrol. 2002; 256(3-4):147–165.
34. Kantz H., Schreiber T. Nonlinear time series analysis. Cambridge Univ. Press, 2003.
35. Sobottka M., de Oliveira L.P.L. Periodicity and predictability in chaotic systems. Amer. Math. Monthly. 2006; 113(5):415-424.
36. Fraser A.M., Swinney H.L. Independent coordinates for strange attractors from mutual information. Phys. Rev. A. 1986; 33(2):1134.
37. Bradley E., Kantz H. Nonlinear time-series analysis revisited. Int. J. Nonlinear Sci. 2015; 25(9):1-11.
38. Abarbanel H. Analysis of observed chaotic data. Springer; 1996.
39. Mayora-Cebollero C., Mayora-Cebollero A., Lozano Á., Barrio R. Full Lyapunov exponents spectrum with deep learning from single-variable time series. Phys. D: Nonlinear Phenom. 2025; 472:134510.
40. Ayers D., Lau J., Amezcua J., Carrassi A., Ojha V. Supervised machine learning to estimate instabilities in chaotic systems: Estimation of local Lyapunov exponents. Q. J. R. Meteorol. Soc. 2023; 149(753): 1236-1262.
41. Milly P.C.D., Wetherald R.T., Dunne K.A., Delworth T.L. Increasing risk of great floods in a changing climate. Nature.2002; 415(6871): 514-517.
42. Kangrang A., Pakoktom W., Nuannukul W., Chaleeraktrakoon C. Adaptive reservoir rule curves by optimisation and simulation. P. I. Civil Eng-Wat. M. 2017; 170(5): 219–230.
43. Kratzert F., Klotz D., Brenner C., Schulz K., Herrnegger M. Rainfall--runoff modelling using Long Short-Term Memory (LSTM) networks. Hydrol. Earth Syst. Science. 2018; 22(11): 6005–6022.
44. Mosavi A., Ozturk P., Chau K., Flood prediction using machine learning models: Literature review. WATER 2018; 10(11): 1536.
45. Songsaengrit S., Kangrang, A. Dynamic rule curves and streamflow under climate change for multipurpose reservoir operation using honey-bee mating optimization. Sustainability 2022; 14(14): 8599.